Asian Journal of Chemistry; Vol. 25, No. 7 (2013), 3579-3582

ASIAN JOURNAL OF CHEMISTRY

http://dx.doi.org/10.14233/ajchem.2013.13658

Preparation and Study on Electrochemical Performance of High-Rate $LiFePO_4$/C Cathode Material

ZHI-PENG MA[1], GUANG-JIE SHAO[1,2,*], WEI WANG[1] and CHUN-YING ZHANG[1]

[1]College of Environmental and Chemical Engineering, Yanshan University, 438 Hebei Street, Qinhuangdao 066004, Hebei, P.R. China
[2]State Key Laboratory of Metastable Materials Science and Technology, Yanshan University, 438 Hebei Street, Qinhuangdao 066004, Hebei, P.R. China

*Corresponding author: Tel/Fax: +86 335 8061569; E-mail: shaogj145@163.com

(*Received*: 27 February 2012; *Accepted*: 4 January 2013) AJC-12652

Carbon-coated $LiFePO_4$ was synthesized by secondary ball-milling method. The structure of the material was systematically studied by X-ray diffraction and field-emission scanning electron microscopy. The particle size of the obtained $LiFePO_4$/C composites was less than 300 nm and the tap density of the $LiFePO_4$/C composites was 1.82 g/cm^3. The electrochemical performance of the material was examined by cyclic voltammetry, electrochemical impedance spectra and constant current charge-discharge testing. The average discharge capacities of the $LiFePO_4$/C composites were 133.4, 125.6, 114.2 and 94 mAh/g at rates of 1C, 2C, 5C and 10C, respectively. Even at 20C rate, the $LiFePO_4$/C composites also showed the average discharge capacity of 81.3 mAh/g.

Key Words: Li-ion battery, $LiFePO_4$/C, High-rate performance.

INTRODUCTION

Olivine-type $LiFePO_4$ is one of the most promising cathode materials for next-generation lithium-ion batteries in large-size and high-rate applications such as electric vehicles (EVs) and hybrid-electric vehicles (HEVs)[1]. It possesses excellent chemical and thermal stability, a high theoretical rate capacity of 170 mAh/g and it offers economic and environmental advantages because it is low cost and nontoxic materials[2-8]. However, the bulk of $LiFePO_4$ has a poor electronic conductivity (*ca.* 10^{-9}-10^{-10} S cm^{-1})[9] and a low lithium diffusion constant (*ca.* 10^{-14}-10^{-16} cm^2 s^{-1})[10]. A poor electronic conductivity and a low lithium diffusion constant in electrodes lead to the discharge capacity of $LiFePO_4$ at high-rate decrease due to lithium diffusion limitation and ohmic drop.

Recently, great progress has been made in enhancing the electrode capacity, rate capability and electrochemical performance of $LiFePO_4$ materials through various synthetic methods and analytical techniques. Fey *et al.*[11] reported that the $LiFePO_4$/C composites were generally synthesized using a high temperature solid-state method and the rate performance has obviously improved. A co-precipitation method combined with a solid-state method has been developed to synthesize double carbon-coated $LiFePO_4$ whose discharge capacity was 120 mAh/g at 10C rate[12]. The high-rate $LiFePO_4$/C cathode material has also been prepared through hydrothermal reactions[13]. The $LiFePO_4$/C with ultrafast charging and discharging has been reported[14], but the performance of this material is doubted[15].

In this work, the $LiFePO_4$/C composites were prepared by secondary ball-milling combined with solid-state method. Our aim was to improve the electrochemical performance of this material, especially its high-rate lithium intercalation/deintercalation properties and tap density.

EXPERIMENTAL

The $LiFePO_4$/C composites were synthesized by secondary ball-milling solid-state reaction using iron oxide [Fe_2O_3], lithium dihydrogen orthophosphate [LiH_2PO_4] and citric acid [$C_6H_8O_7 \cdot H_2O$] as carbon source. The mixture was ball-milled for 5 h and heated at 700 ºC for 12 h under nitrogen atmosphere in order to obtain the bare $LiFePO_4$. Superfluous citric acid was added to the bare sample. Eventually, carbon-coated $LiFePO_4$ composites were synthesized by ball-milling the mixture for 6 h and heating it at 700 ºC for 4 h under nitrogen atmosphere.

The crystal structure of the $LiFePO_4$/C composites was evaluated by X-ray diffraction method using CuK_α radiation (Rigaku D-max-2500/PC). The X-ray diffraction data were detected in the angle interval form 15-55º (2θ) at steps of 5º (2θ). The particle size of the $LiFePO_4$/C composites was observed by field-emission scanning electron microscopy (HITACHI S-4800).

The electrode was fabricated by dispersing 80 wt % active material, 10 wt % polyvinylidene fluorid (PVDF) and 10 wt % acetylene black in N-methy1-2-pyrrolidone (NMP) in order to form the slurry. The slurry was then spread onto an Al foil substrate and then dried for 12 h at 120 ºC in a vacuum drying oven to obtain the cathode film. The cathode was formed by cutting into a circular disc and weighted. The cells were assembled using the lithium metal foil negative electrode, the $LiFePO_4$/C positive electrode, the microporous polypropylene separator (Celgard 2004) and the electrolyte of 1 M $LiPF_6$ in 1:1 EC/DMC inside a glove box filled with argon gas. The cells were charged at identical rates and discharged at various rates. The voltage range of the cells tested was between 4.2 and 2.4 V.

RESULTS AND DISCUSSION

Fig. 1 shows the X-ray diffraction (XRD) patterns of the $LiFePO_4$/C composites. The relative intensity and positive diffraction of the $LiFePO_4$/C sample are indexed to $LiFePO_4$ and no impurity peak in the sample is detected by X-ray diffraction measurements. No carbon diffraction peak is detected in Fig. 3. Therefore, it means that the carbon-coated also does not affect the crystal structure of $LiFePO_4$ and the synthesized $LiFePO_4$ powers have high purity.

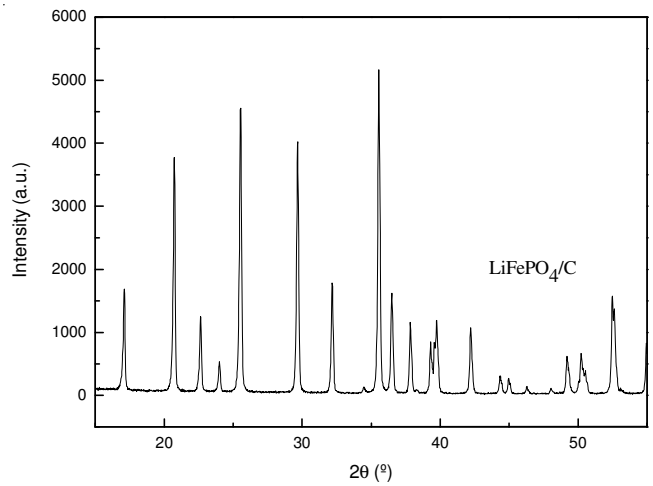

Fig. 1. X-Ray diffraction patterns for the $LiFePO_4$/C composites

The particle size of the material is an extremely important factor for the electrochemical property of the battery material, especially its high-rate charger-discharger performance. Fig. 2 shows the FE-SEM image of the pure $LiFePO_4$, $LiFePO_4$/citric-acid and $LiFePO_4$/C, respectively. It is apparent from Fig. 2(a) that the particle of the pure $LiFePO_4$ is reunited, however, Fig. 2(c) displays that the synthesized $LiFePO_4$/C powders by a high-energy secondary ball-milling are mainly particles between 100 and 300 nm in size, although a few large particles up to 1 μm exist. The particles of the $LiFePO_4$/C composites have a similar spherical morphology and carbon is uniformly coated on the surface of $LiFePO_4$. The material has a high tap density, because the gap of large particles is filled in smaller particles. The measured tap density is 1.82 g cm^{-3}, this high tap density is great importance to the practical application in lithium batteries, because it ensures a high volumetric energy density.

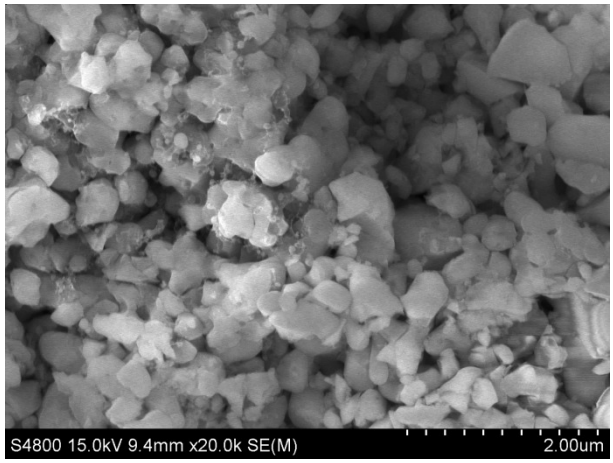

(a)

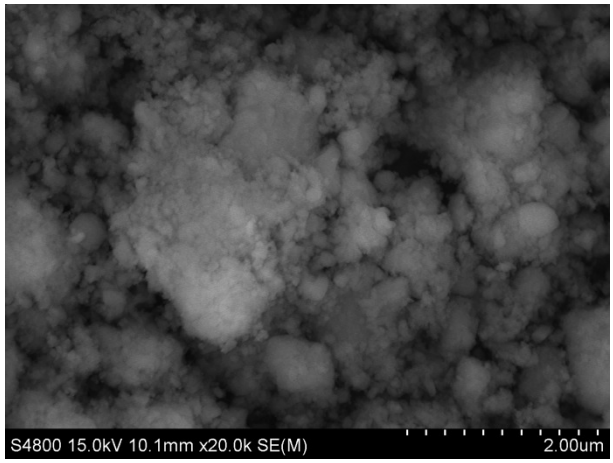

(b)

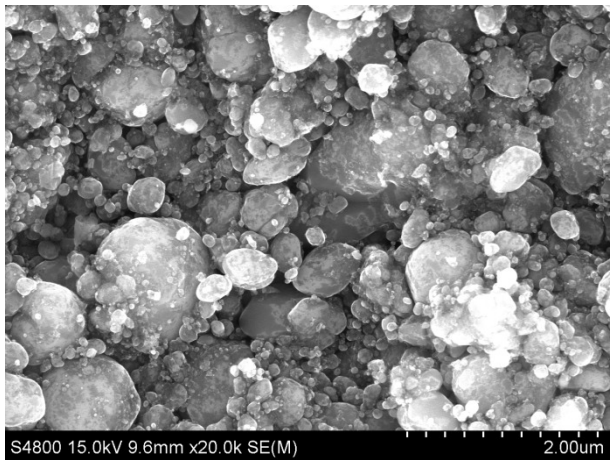

(c)

Fig. 2. FE-SEM image of (a) $LiFePO_4$, (b) $LiFePO_4$/citric acid and (c) $LiFePO_4$/C

Fig. 3 shows the rate performance of $LiFePO_4$/C composites at various discharge rates. The average discharge capacities of the $LiFePO_4$/C composites were 133.4, 125.6, 114.2 and 94 mAh/g at rates of 1C, 2C, 5C and 10 C, respectively. Even at 20C rate, the $LiFePO_4$/C composites also showed the average discharge capacity of 81.3 mAh/g. It is concluded that the secondary ball-milling method can improve the high-rate performance of the $LiFePO_4$/C materials, because the

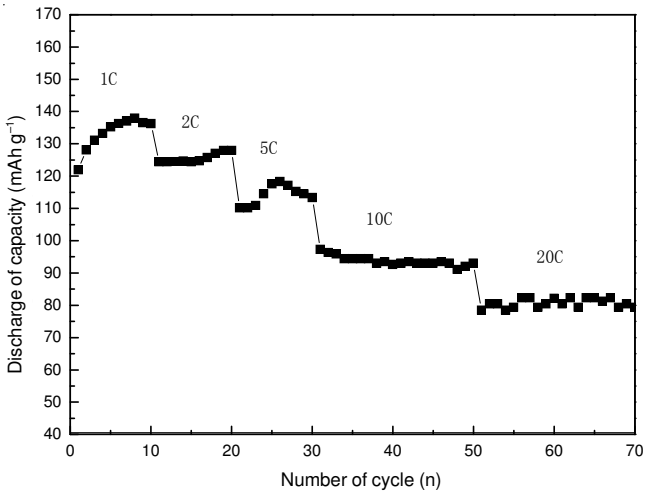

Fig. 3. Discharge capacities of at various rates

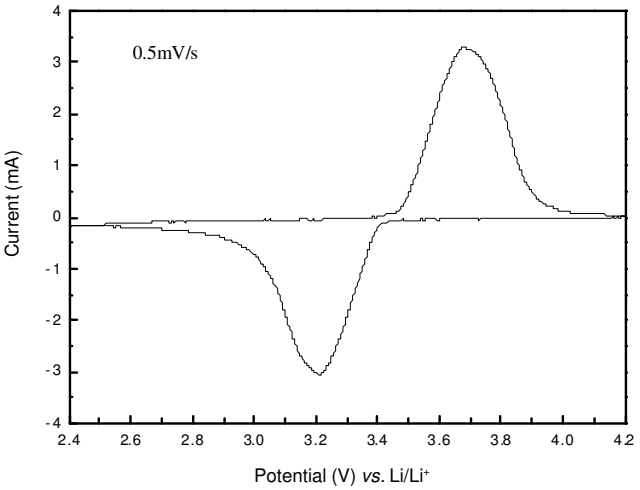

Fig. 5. Cyclic voltammograms of the $LiFePO_4$/C electrode material lithium can act as reference and counter electrodes between 2.4 and 4.2 V with the scanning rate of 0.5 V/s

secondary ball-milling method refined the grain size of the bare $LiFePO_4$ and shortened the transport path of Li^+ and improved its transfer. Fig. 4 shows the galvanostatic charge-discharge performance of a Li/$LiFePO_4$ half-cell at 1C rate. The half-cell exhibits the typical voltage plateau along 3.5 V (*vs.* Li) associated with the Fe^{2+}/Fe^{3+} redox processes. The capacity delivery is equal to 134.3 mAh/g for charge and 135.2 mAh/g for discharge. In addition, the voltage profiles show a narrow gap between charge and discharge, indicating very low electrode resistance. These factors would improve the electrochemical performance of the $LiFePO_4$/C materials, especially, high-rate capacity.

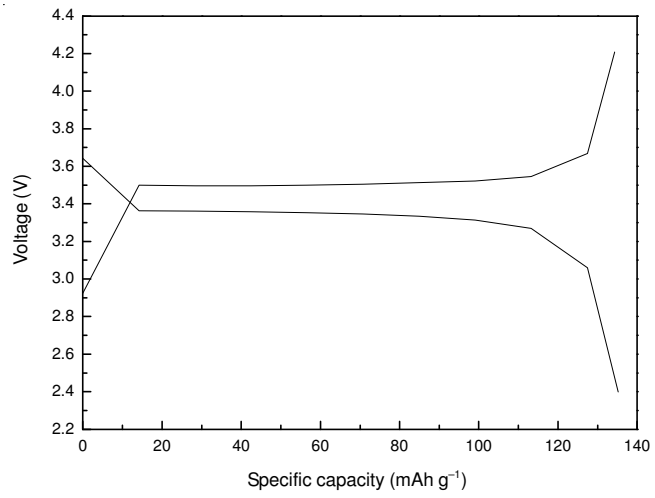

Fig. 4. Voltage profile of the charge-discharge cycle of Li/$LiFePO_4$ half-cell at 1C rate

Fig. 5 reports cyclic voltammetry curve of 20 cycles of the preparing $LiFePO_4$/C electrode material at 0.5 m V/s scanning rate. The well defined sharp redox peaks at 3.68 V (anodic peak) and 3.214 V (cathodic peak) should be attributed to the Fe^{2+}/Fe^{3+} redox couple reaction, corresponding to lithium-ion extraction and insertion in $LiFePO_4$ crystal structure. The voltage margin between anodic peak and cathodic peak was 0.466 V, this explained that the reversibility of the $LiFePO_4$/C electrode material was significantly improved. The phase change of the $LiFePO_4/FePO_4$ could minish the crystal cell volume of the $LiFePO_4$, because the Fe^{3+} ionic radius is smaller than the Fe^{2+} ionic radius. Lithium-ion transfer was embarrassed by its phase change. However, the smaller grain size of the $LiFePO_4$/C improved lithium-ion transfer and shortened the transport path of lithium-ion.

Fig. 6 shows the electrochemical impedance spectra (EIS) of the $LiFePO_4$/C electrode material after 20 cycles at fully discharge in the frequency range from 10 mHz to 100 KHz. The EIS is composed of three partially overlapped two semicircles in the high frequency region and a straight line in the low frequency region. An intercept at the Z_{re} axis in the high frequency region corresponds to the bulk ohmic resistance of the electrolyte (R_e) in the equivalent circuit showed in Fig. 7. The semicircle in the high frequency region represents the migration of the lithium-ion through the solid electrolyte interphase (SEI) layer at the electrode/electrolyte interface and it corresponds to the R_f in the equivalent circuit and it corresponds to the diameter of this semicircle. The semicircle in the middle-high frequency range indicates the charge transfer resistance (R_{ct}) in the equivalent circuit and it corresponds to the diameter of this semicircle. The straight line in the low frequency region represents the Warburg impedance (Z_w) in the equivalent circuit, which is attributed to the diffusion of the lithium-ion in the bulk of the electrode material. A constant phase element CPE is placed to represent the double layer capacitance and passivation film capacitance[16]. The capacitance resistance is to small that negligible. The fitting results were analyzed using Zview-Impedance 2.80 software. The bulk ohmic resistance of the electrolyte (R_e), the resistance of surface film (R_f) and the charge transfer resistance (R_{ct}) were 10.8, 10.89 and 16.85 Ω, respectively. The charge transfer resistance is related to complex reaction of charge transfer process between the electrolyte and the active materials[17,18]. The smaller charge transfer resistance indicates that lithium-ion and electron transfer are more feasible on the electrode and is benefit to overcome the restriction of kinetics in the charge-discharge process and improve the electrochemical activity of the material by ameliorating the preparing method of the $LiFePO_4$/C composites. An exchange current density

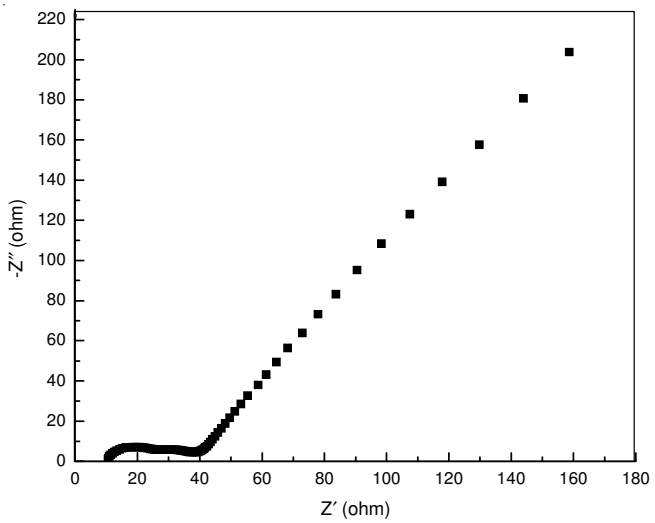

Fig. 6. Electrochemical impedance spectra of the $LiFePO_4$/C composites

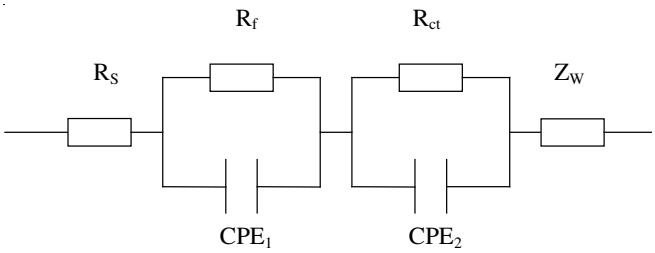

Fig. 7. Equivalent circuit for fitting experimental EIS data

(I_0) is an important parameter of kinetics for an electrochemical reaction and can measure the catalytic activity of electrodes. It was calculated using the following formula.

$$I_0 = \frac{RT}{nR_{ct}F} \quad (1)$$

where R is the gas constant, T is the absolute temperature, n is the charge transfer number, R_{ct} is the charge transfer resistance and F is the Faraday constant.

The value of the exchange current density (I_0) was 1.498 mA/g. The larger value implies that the electrochemical catalytic activity of the preparing $LiFePO_4$/C material by secondary ball-milling method is higher. This is the reason why the $LiFePO_4$/C composite has the well high-rate performance.

Conclusion

The $LiFePO_4$/C composites were synthesized by the secondary ball-milling high temperature solid-state reaction method under nitrogen atmosphere and their electrochemical performance were investigated. Studies *via* FE-SEM analyses can provide insight into the morphology of the $LiFePO_4$/C on a nanoscopic scale, which seems closely related to the preparation process of the samples. The particle size of the obtained $LiFePO_4$/C composites was less than 300 nm. The tap density of the $LiFePO_4$/C was 1.82 g/cm^3, which is greatly important to guarantee the high volumetric energy density of lithium batteries in practical application. The $LiFePO_4$/C composites were constructed with the great mass of carbon film covered with the surface of $LiFePO_4$. The $LiFePO_4$/C cathode composites delivered the high average discharge capacities of 133.4, 125.6, 114.2 and 94 mAh/g at rates of 1C, 2C, 5C and 10C, respectively. Even at 20C rate, it also showed the average discharge capacity of 81.3 mAh/g. The homogeneous microstructure of the $LiFePO_4$/C composites led to an increase in an electronic conductivity by close contact of the $LiFePO_4$/C interface. Therefore, the $LiFePO_4$/C composites with better homogeneous microstructure and narrow particle size distribution are chief requirements in the study on electrochemical performance of this material.

REFERENCES

1. M. Yonemura, A. Yamada, Y. Takei, N. Sonoyama and R. Kanno, *J. Electrochem. Soc*., **151**, A1352 (2004).
2. A.K. Padhi, K.S. Nanjundaswamy and J.B. Goodenough, *J. Electrochem. Soc*., **144**, 1188 (1997).
3. G.W. Wang, S. Bewlay. J. Yao, J.H. Ahn, S.X. Dou and H.K. Liu, *Electrochem. Solid State Lett*., **7**, A503 (2004).
4. C.M. Julien, K. Zaghib, A. Mauger, M. Massot, A. Ait-Salah, M. Selmane and F. Gendron, *J. Appl. Phys*., **100**, 063511 (2006).
5. G. Xiao-Dong, Z. Ben-He, T. Hong, T. Yan, Z. Yan-Jun and S. Yang, *Asian J. Chem*., **23**, 3837 (2011).
6. F. Sauvage, E. Baudrin, L. Gengembre and J.M. Tarascon, *Solid State Ionics*, **176**, 1869 (2005).
7. D.D. MacNeil, Z. Lu, Z. Chen and J.R. Dahn, *J. Power Sources*, **108**, 8 (2002).
8. M. Takahashi, S.I. Tobishima, K. Takei and Y. Sakurai, *Solid State Ionics*, **148**, 283 (2002).
9. S.Y. Chung, J.T. Bloking and Y.M. Chiang, *Nat. Mater*., **1**, 123 (2002).
10. P.P. Prosini, M. Lisi, D. Zane and M. Pasquali, *Solid State Ionics*, **148**, 45 (2002).
11. G.T.K. Fey and T.L. Lu, *J. Power Sources*, **178**, 807 (2008).
12. S.W. Oh, S.T. Myung, S.M. Oh, K.H. Oh, K. Amine, B. Scrosati and Y.K. Sun, *Adv. Mater*., **22**, 4842 (2010).
13. A. Kuwahara, S. Suzuki and M. Miyayama, *Ceram. Int*., **34**, 863 (2008).
14. B. Kang and G. Ceder, *Nature*, **458**, 190 (2009).
15. K. Zaghib, J.B. Goodenough, A. Mauger and C. Julien, *J. Power Sources*, **194**, 1021 (2009).
16. G.X. Wang, L. Yang, Y. Chen, J.Z. Wang, S. Bewlay and H.K. Liu, *Electrochim. Acta*, **50**, 4649 (2005).
17. J.L. Liu, R.R. Jiang, X.Y. Wang, T. Huang and A.S. Yu, *J. Power Sources*, **194**, 536 (2009).
18. J. Molenda, W. Ojczyk and J. Marzec, *J. Power Sources*, **174**, 689 (2007).